



Universal Current-Mode Filters Based on OTA and MO-CCCA

Yi Li, Chunhua Wang, Baihui Zhu & Zhenhua Hu

To cite this article: Yi Li, Chunhua Wang, Baihui Zhu & Zhenhua Hu (2017): Universal Current-Mode Filters Based on OTA and MO-CCCA, IETE Journal of Research, DOI: [10.1080/03772063.2017.1381575](https://doi.org/10.1080/03772063.2017.1381575)

To link to this article: <https://doi.org/10.1080/03772063.2017.1381575>



Published online: 06 Dec 2017.



Submit your article to this journal [↗](#)



Article views: 15



View Crossmark data [↗](#)

Universal Current-Mode Filters Based on OTA and MO-CCCA

Yi Li, Chunhua Wang, Baihui Zhu and Zhenhua Hu

Department of Communication Engineering, College of Computer Science and Electronic Engineering, Hunan University, Changsha, P. R. China

ABSTRACT

In this paper, a new universal current-mode filtering circuit with single input and multi-outputs based on OTAs (operational transconductance amplifiers) is proposed. The circuit just consists of two operational transconductance amplifiers, one current controlled current amplifier with multi-outputs (MO-CCCA), and two grounded capacitors. It can realize low-pass, band-pass, high-pass, band-stop, and all-pass filters simultaneously. Its quality factor and natural frequency can be tuned independently and the sensitivities are very low. Moreover, the non-ideal characteristic of the proposed filter is analysed and simulated by PSPICE.

KEYWORDS

Current-mode circuit; Filter; Operational transconductance amplifier

1. INTRODUCTION

Recently, the applications and advantages in the realization of high performance current-mode active filters have received considerable attentions. It is well known that operational transconductance amplifiers (OTAs) provide highly linear electronic tunability, very wide tuning range of transconductance and frequency range. So, OTA is a very good basic block to design high performance current-mode filters.

A biquad filter is very useful block to realize high-order filters. Some current-mode biquad filtering circuits based on OTA have been reported. The filters may be divided into subcategories considering the input and output ports: (i) single input and single output (SISO) [1–3]; (ii) multi-inputs and single output (MISO) [4,5]; (iii) multi-inputs and multi-outputs (MIMO) [6–9]; (iv) single input and multi-outputs (SIMO) [10–21]. The SISO filters can realize multi-function outputs by altering the connection way of the circuits, but altering the connection way can only realize a filtering output at a time. In [1], the SISO filter which employs 11 OTAs, 1 current controlled current differencing current conveyor, 4 grounded capacitors, and two resistors is proposed. Although this filter possesses independent tunability of ω_0 and Q , the number of components is too many to restrict its application. The MISO filters imply that only one filter function can be realized at a time. The MIMO filters can realize multifunction outputs simultaneously, but they need input signal matching. The SIMO filters can simultaneously realize second-order low-pass, band-pass, high-pass, band-stop, and all-pass filters at a time without altering the connection

way of the circuits and without input signal matching, it plays an important role in the fields of electronic measurement, communication, auto control, and nerve network. A good SIMO current-mode filter should enjoy the following features:

- (I) Capability of realizing the five filtering functions (low-pass, band-pass, high-pass, band-stop, and all-pass) and without any matching conditions or component choice;
- (II) Simple circuit structure (three active elements and two grounded capacitors);
- (III) Grounded capacitors;
- (IV) Capability of realizing explicitly current outputs without the need of any additional elements;
- (V) Independent tunability of ω_0 and Q .

Investigation on the recently proposed SIMO current-mode OTA-based filters shows that none of these exhibit the all the above features. A comparison of the features of the recently reported filters is given in Table 1. The table contains references which are from [10] to [26]. For example, the filter proposed in [10] has the features (I), (III), and (IV), but it does not satisfy features (II) and (V) since it employs four active components. In [10], the quality factor and natural frequency cannot be adjusted independently, and the band-stop and all-pass functions are realized by adding low-pass signal, high-pass signal, and band-pass signal, so strictly speaking, the filter cannot be called SIMO filter. The filter in [11] satisfies all the above

Table 1: Comparison of the performance parameters of recently reported OTA based filters

Circuit reference	(I)	(II)	(III)	(IV)	(V)
[10]	Yes	No	Yes	Yes	No
[11]	Yes	Yes	No	Yes	No
[12]	Yes	No	Yes	Yes	Yes
[13]	No	No	No	Yes	Yes
[14]	Yes	No	Yes	Yes	No
[15]	No	No	No	Yes	Yes
[16]	Yes	No	No	Yes	Yes
[17]	No	Yes	Yes	Yes	Yes
[18]	No	No	No	Yes	Yes
[19]	Yes	No	Yes	Yes	Yes
[20]	Yes	No	Yes	Yes	Yes
[21]	Yes	No	Yes	Yes	Yes
[22]	Yes	Yes	Yes	Yes	Yes
[23]	Yes	No	Yes	Yes	Yes
[24]	Yes	No	Yes	Yes	Yes
[25]	Yes	No	Yes	Yes	Yes
[26]	No	No	Yes	Yes	No

features except features (III) and (V). Although the number of components is low, the capacitors are not grounded which are not suitable for IC integration, and the output of high-pass could not provide high output impedance. In addition, the band-stop and all-pass functions are realized by adding other output signals with different function as well. The filter in [12] could not get the feature (II), which results in the complex structure, more power consumption, and more area of chip. In [13], six kinds of the SIMO filters which get the features (IV) and (V) have been proposed, however, each filter could not realize the low-pass, band-pass, high-pass, band-stop, and all-pass five filtering functions, and have the problem of too many number of components used in each filter. In [22], although the five features are achieved, however, the natural frequency ω_0 in [22] is shown as $\sqrt{1/(R_{X1}R_{X2}C_1C_2)}$, because tuning range of the parasitic resistance (R_{X1} and R_{X2}) of CCCII is small,

the tuning range of natural frequency ω_0 is small. In [23], the universal filter is formed by four active CCCII which cannot satisfy feature (II). In [24], the natural frequency ω_0 is written as $\sqrt{R_1R_2C_1C_2}$ which is adjusted by passive elements, so it could not be adjusted flexibly by external bias voltage or current. On the other hand, the filter contains additional four resistors in [24], which means that it could not achieve the feature (II). In [25], the filter employs additional one resistor. So, the work also could not gain the feature (II). In [26], although each of the filters only uses one active component, it could realize only two kinds of functions which are low-pass and band-pass. Through the connection of low-pass and band-pass outputs, additional one function which is high-pass could be got. In addition, its natural frequency and quality factor could not be adjusted independently. So, the filter in [26] could not get the features (I), (II), and (V).

In this paper, a new universal single-input multi-output filtering circuit is proposed, which just three active components (two OTAs and one MO-CCCA) and two grounded capacitors are employed. It can realize low-pass, band-pass, high-pass, band-stop, and all-pass filtering outputs simultaneously without element matching condition. The characteristic parameters ω_0 and Q can be adjusted independently by bias current of MO-CCCA. It satisfies all the above five features. The sensitivities are very low.

2. THE CIRCUIT SYMBOL OF MO-CCCA AND ITS REALIZATION CIRCUIT

Figure 1(a) denotes the symbol of MO-CCCA, where i represents input, o_1 - o_n are n outputs respectively, K is

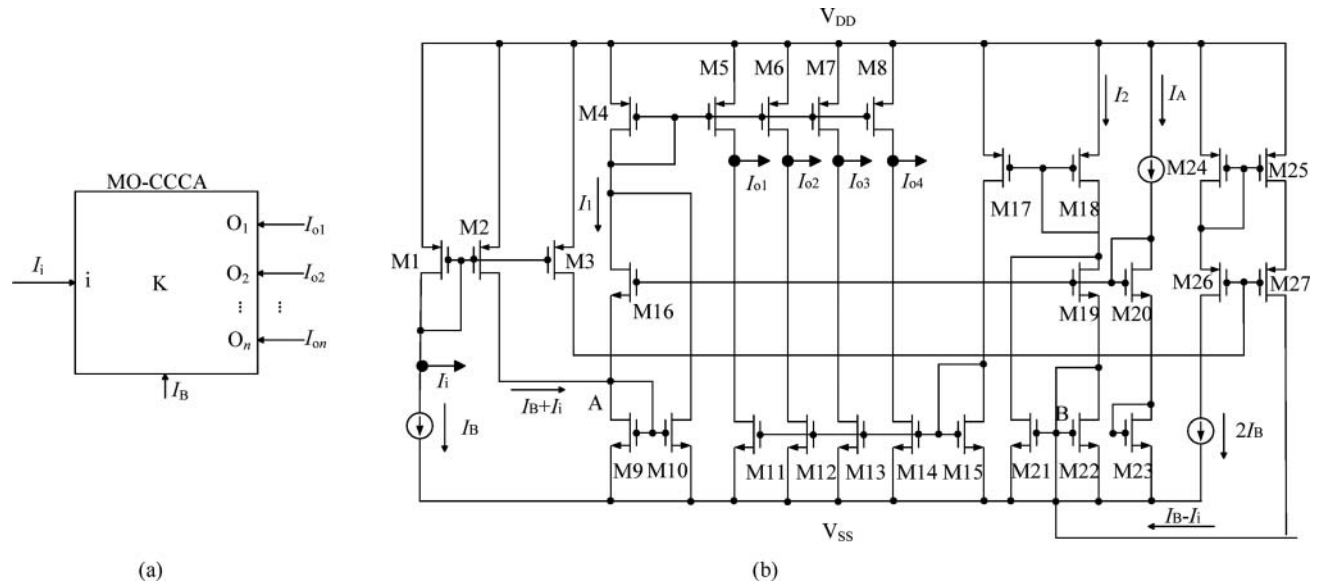


Figure 1: (a) MO-CCCA symbol (b) MO-CCCA realization circuit

current gain, I_B denotes bias DC current which can be adjusted to change K . Figure 1(b) is the realization circuit [27]. I_i denotes input signal; I_{o1} , I_{o2} , I_{o3} , I_{o4} are four outputs, respectively. Transistors (M9, M10, M16) and (M19, M21, M22) constitute two square root circuits whose inputs are point A and point B, respectively. Due to that M1–M3 form a basic current mirror and M24–M27 form a cascade current mirror, the drain current of M2 (namely input current of point A) is equal to $I_B + I_i$, the drain current of M27 (namely input current of point B) is equal to $I_B - I_i$. The current source I_A , transistor M20, and transistor M23 form bias circuit which provides bias voltage for M16 and M19. All MOS transistors operate in saturation range. The current I_1 of M4 and current I_2 of M18 are shown in (1) and (2), respectively [28]:

$$I_1 = 2I_A + (I_B + I_i)^2 / (8I_A) \quad (1)$$

$$I_2 = 2I_A + (I_B - I_i)^2 / (8I_A) \quad (2)$$

If the channel size of M5–M8 are all n times that of M4, and the channel size of M17 are n times that of M18, $(W/L)_{M5}/(W/L)_{M4} = (W/L)_{M6}/(W/L)_{M4} = (W/L)_{M7}/(W/L)_{M4} = (W/L)_{M8}/(W/L)_{M4} = (W/L)_{M17}/(W/L)_{M18} = n$, the output currents can be obtained in the following equation:

$$I_{O1} = I_{O2} = I_{O3} = I_{O4} = (nI_B/2I_A)I_i = KI_i \quad (3)$$

where K denotes current gain. It is clear from (3) that K can be set by I_B .

3. PROPOSED CURRENT-MODE FILTERING CIRCUIT AND ANALYSIS

The proposed circuit is shown in Figure 2 which contains two OTAs, one MO-CCCA, and two grounded capacitors. I_{in} is input current signal, and I_{o1} , I_{o2} , I_{o3} , I_{o4} ,

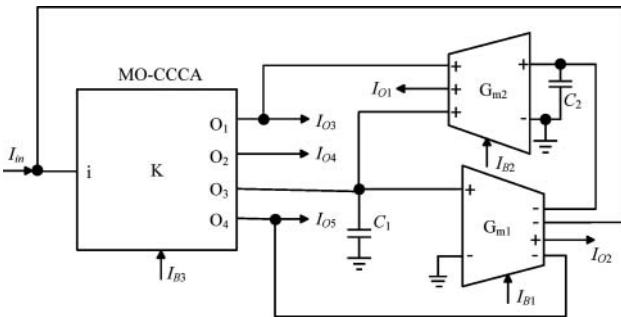


Figure 2: The proposed filtering circuit

I_{o5} represent five outputs, respectively. According to the port characteristic of OTA, analysing Figure 2 yields following current transfer functions as (4)–(8):

$$T_{LP}(S) = \frac{I_{o1}}{I_{in}} = \frac{KG_{m1}G_{m2}}{S^2C_1C_2 + SC_2G_{m1}K + G_{m1}G_{m2}} \quad (4)$$

$$T_{BP}(S) = \frac{I_{o2}}{I_{in}} = \frac{SC_2G_{m1}K}{S^2C_1C_2 + SC_2G_{m1}K + G_{m1}G_{m2}} \quad (5)$$

$$T_{HP}(S) = \frac{I_{o3}}{I_{in}} = \frac{S^2KC_1C_2}{S^2C_1C_2 + SC_2G_{m1}K + G_{m1}G_{m2}} \quad (6)$$

$$T_{BS}(S) = \frac{I_{o4}}{I_{in}} = K \frac{S^2C_1C_2 + G_{m1}G_{m2}}{S^2C_1C_2 + SC_2G_{m1}K + G_{m1}G_{m2}} \quad (7)$$

$$T_{AP}(S) = \frac{I_{o5}}{I_{in}} = K \frac{S^2C_1C_2 - SC_2G_{m1} + G_{m1}G_{m2}}{S^2C_1C_2 + SC_2G_{m1}K + G_{m1}G_{m2}} \quad (8)$$

It is clear from (4)–(8) that I_{o1} is low-pass output, I_{o2} is band-pass output, I_{o3} is high-pass output, I_{o4} is band-stop output, and I_{o5} is all-pass output ($K = 1$). The natural frequency and quality factor are shown in the following equation:

$$\omega_0 = \sqrt{\frac{G_{m1}G_{m2}}{C_1C_2}} \quad Q = \frac{1}{K} \sqrt{\frac{C_1G_{m2}}{C_2G_{m1}}} \quad (9)$$

From (9), it can be seen that adjusting G_{m1} , G_{m2} simultaneously, we can adjust the parameter ω_0 without disturbing Q . The parameter Q can also be adjusted by K without disturbing ω_0 . Therefore, the biquad filter has independently tuning capability for the characteristic parameters ω_0 and Q .

Based on the sensitivities expression: $S'_x = (x/y) \times (\partial y / \partial x)$, according to (9), we can calculate the sensitivities which are $S_{G_{m1}, G_{m2}}^{\omega_0} = -S_{C_1, C_2}^{\omega_0} = 1/2$, $S_{G_{m2}, C_1}^Q = -S_{G_{m1}, C_2}^Q = 1/2$, $S_k^Q = -1$. It is clear that the proposed filter circuits bear low sensitivities.

4. INFLUENCE OF PARASITIC ELEMENT DISCUSSION

As is shown Figure 1(b), the MO-CCCA input stage is formed by transistors M1 and M2 according to small-signal equivalent circuit of NMOS transistor [29]. Considering the small-signal characteristics in high frequency, the whole small-signal equivalent circuit of MO-CCCA input

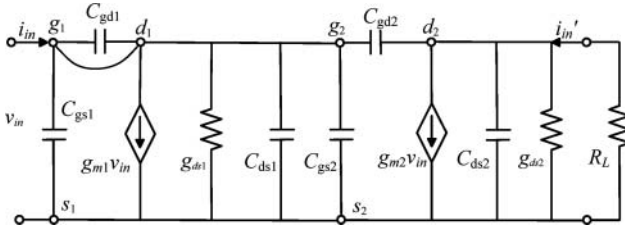


Figure 3: The whole small-signal equivalent circuit of the MO-CCCA input stage

stage is shown in Figure 3, where $C_{gs1,2}$, $C_{gd1,2}$, and $C_{ds1,2}$ are gate-source, gate-drain, and drain-source capacitors of transistors M1,2 respectively, $g_{m1,2}v_{in}$ are current source controlled by v_{in} , $g_{ds1,2}$ are drain-source conductance of transistors M1,2. The small-signal equivalent circuit of the MO-CCCA input stage (M1–M2) is shown in Figure 3 which can be transformed to Figure 4, here, $C_1' = C_{gs1} + C_{gs2} + C_{ds1}$, $C_2' = C_{gd2}$, $C_3' = C_{ds2}$.

The current gain transfer function in Figure 4 can be obtained as (10), the detailed deduction is shown in the Appendix:

$$\begin{aligned} \frac{i_{in}'}{i_{in}} &= \frac{g_{m2} - sC_2'}{s(C_1' + C_2') + g_{m1} + 1/r_{ds1}} \\ &= \frac{g_{m2} - sC_2'}{s(C_1' + C_2') + g_{m1} + g_{ds1}} \end{aligned} \quad (10)$$

The real MO-CCCA exhibits parallel equivalent parasitic impedances at the output terminals, similarly, the real OTA exhibits a parallel equivalent parasitic impedance between every port and the ground. Considering the influence of the parasitic elements in OTA and MO-CCCA, the proposed filter shown in Figure 2 can be transformed to Figure 5, where Z_1 is impedance of C_1 and the parasitic elements, and Z_2 is that of C_2 and the parasitic elements.

We define R_{02} , C_{02} as the parasitic resistor and capacitor of the output terminal of MO-CCCA, R_{11} , C_{11} and R_{21} , C_{21} as the input terminal parasitic elements of the first and the second OTAs, R_{12} , C_{12} and R_{22} , C_{22} as the

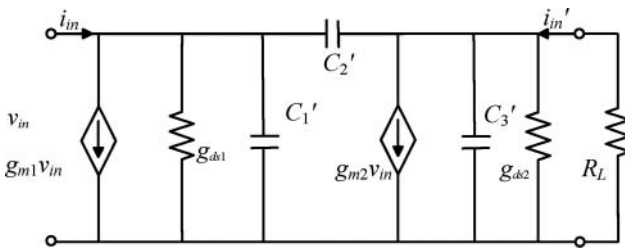


Figure 4: Small-signal equivalent circuit of the MO-CCCA input stage

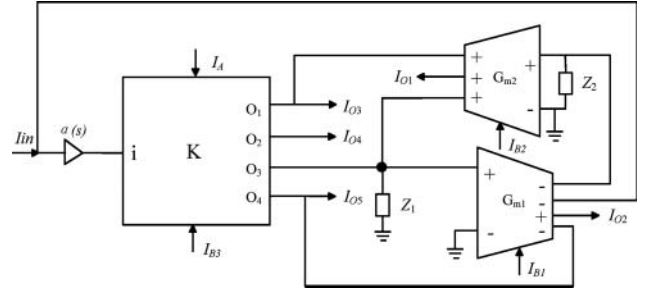


Figure 5: Proposed filter including parasitic elements of the OTA and MO-CCCA

parasitic elements of the two OTAs at the output terminals. Assuming that $\min(C_1, C_2) \gg (C_1' + C_2' + C_{02} + C_{11} + C_{12} + C_{21} + C_{22})$, $C_{22} \gg (C_1' + C_2')$, we can get that

$$\begin{aligned} Z_1 &= (R_{02} // R_{11} // R_{22}) // (C_1 // C_{02} // C_{11} // C_{22}) \\ &\approx (R_{02} // R_{22}) // C_1 = R // C_1 = \frac{R}{1 + sC_1 R} \end{aligned} \quad (11)$$

$$\begin{aligned} Z_2 &= (R_{12} // R_{21}) // (C_2 // C_{12} // C_{21}) \\ &\approx R_{12} // C_2 = \frac{R_{12}}{1 + sC_2 R_{12}} \end{aligned} \quad (12)$$

where $R = R_{02} // R_{22}$. To derive the parameter $\alpha(s)$, MO-CCCA associates with the first OTA should be considered. The input terminal of MO-CCCA is connected with the output terminal of the first OTA, the small-signal equivalent circuit shown in Figure 4 can be transformed to Figure 6, here, g_{ds1} is transformed to $g_{ds1} // g_{12}$ and C_1' is transformed to $C_1' // C_{12}$, where g_{12} is output conductance of the first OTA. According to (10), the following equation can be obtained:

$$\begin{aligned} \alpha(s) &= \frac{i_{in}'}{i_{in}} = \frac{g_{m2} - sC_2'}{s(C_1' // C_{22} + C_2') + g_{m1} + g_{ds1} // g_{22}} \\ &\approx \frac{g_{m2} - sC_2'}{s(C_{22} + C_2') + g_{m1} + g_{ds1}} \approx \frac{g_{m2} - sC_2'}{sC_{22} + g_{m1} + g_{ds1}} \end{aligned} \quad (13)$$

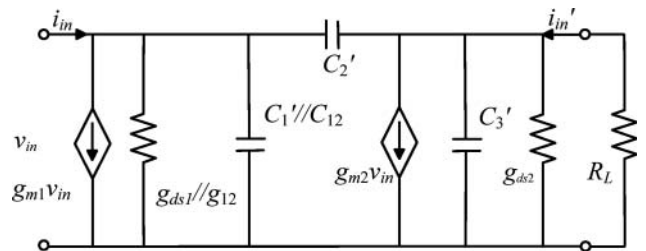


Figure 6: Deduction of $\alpha(s)$

From Figure 5, the following functions can be obtained:

$$\begin{aligned} \frac{I_{O1}}{I_{in}} &= K \frac{\alpha Z_1 Z_2 G_{m1} G_{m2}}{Z_1 Z_2 G_{m1} G_{m2} + K\alpha Z_1 G_{m1} + 1} \\ &= K\alpha \frac{RR_{12} G_{m1} G_{m2}}{D(s)} \end{aligned} \quad (14)$$

$$\begin{aligned} \frac{I_{O2}}{I_{in}} &= K \frac{\alpha Z_1 G_{m1}}{Z_1 Z_2 G_{m1} G_{m2} + K\alpha Z_1 G_{m1} + 1} \\ &= K\alpha \frac{RG_{m1}(1 + sC_2 R_{12})}{D(s)} \end{aligned} \quad (15)$$

$$\begin{aligned} \frac{I_{O3}}{I_{in}} &= K \frac{\alpha}{Z_1 Z_2 G_{m1} G_{m2} + K\alpha Z_1 G_{m1} + 1} \\ &= K\alpha \frac{(1 + sC_1 R)(1 + sC_2 R_{12})}{D(s)} \end{aligned} \quad (16)$$

$$\begin{aligned} \frac{I_{O4}}{I_{in}} &= K \frac{\alpha + \alpha Z_1 Z_2 G_{m1} G_{m2}}{Z_1 Z_2 G_{m1} G_{m2} + K\alpha Z_1 G_{m1} + 1} \\ &= K\alpha \frac{(1 + sC_1 R)(1 + sC_2 R_{12}) + RR_{12} G_{m1} G_{m2}}{D(s)} \end{aligned} \quad (17)$$

$$\begin{aligned} \frac{I_{O5}}{I_{in}} &= K \frac{\alpha Z_1 Z_2 G_{m1} G_{m2} - \alpha Z_1 G_{m1} + \alpha}{Z_1 Z_2 G_{m1} G_{m2} + K\alpha Z_1 G_{m1} + 1} \\ &= K\alpha \frac{(1 + sC_1 R)(1 + sC_2 R_{12}) - RG_{m1}(1 + sC_2 R_{12}) + RR_{12} G_{m1} G_{m2}}{D(s)} \end{aligned} \quad (18)$$

where

$$\begin{aligned} D(s) &= (1 + sC_1 R)(1 + sC_2 R_{12}) \\ &+ K\alpha RG_{m1}(1 + sC_2 R_{12}) + RR_{12} G_{m1} G_{m2} \\ &= s^2 C_1 C_2 RR_{12} + s[C_1 R + C_2 R_{12}(1 + K\alpha RG_{m1})] \\ &+ RR_{12} G_{m1} G_{m2} + K\alpha RG_{m1} + 1 \end{aligned} \quad (19)$$

then, the natural frequency and quality factor can be obtained as

$$\omega_0' = \sqrt{\frac{G_{m1} G_{m2}}{C_1 C_2}} \sqrt{1 + K\alpha/(R_{12} G_{m2}) + 1/(RR_{12} G_{m1} G_{m2})} \quad (20)$$

$$Q' = \frac{1}{K} \sqrt{\frac{C_1 G_{m2}}{C_2 G_{m1}}} \sqrt{\frac{1 + K\alpha/(R_{12} G_{m2}) + 1/(RR_{12} G_{m1} G_{m2})}{\alpha + 1/(KRG_{m1}) + C_1/(KC_2 G_{m1} R_{12})}} \quad (21)$$

It is clear that when considering influence of parasitic elements, the natural angle frequency is higher than the

one in ideal condition, namely $\omega_0' > \omega_0$. Assuming the value of R_{12} is chosen large enough, then $\omega_0' = \omega_0$, and the influence of non-ideal characteristics of OTA and MO-CCCA can be ignored. When R_{12} and R are large enough, (21) can be rewritten as

$$Q' = Q \sqrt{\frac{1}{\alpha}} = Q \sqrt{\frac{sC_{22} + g_{m1} + g_{ds1}}{g_{m2} - sC_2'}} \quad (22)$$

If $g_{m1} = g_{m2}$, and $C_{22} > C_2'$, it is clear that the quality factor is higher than that in the ideal condition.

5. PSPICE SIMULATION RESULTS

To verify the circuit shown in Figure 2, the low-pass, band-pass, high-pass and band-stop, and all-pass filters are simulated in PSPICE using the TSMC CMOS 0.5 μm technology. For the simulations, the OTA circuit used is shown in Figure 7 [30], where V_+ denotes non-inverting (+) input, V_- is inverting (-) input; I_{o1} , I_{o2} , I_{o3} represent non-inverting outputs; \bar{I}_{o1} , \bar{I}_{o2} , \bar{I}_{o3} are inverting outputs; all drain channel sizes are $W/L = 4 \mu\text{m}/2 \mu\text{m}$. For MO-CCCA, the drain channel lengths of all MOS are $L = 2 \mu\text{m}$. The drain channel widths of M5, M6, M7, M8, and M17 are $W = 8 \mu\text{m}$ and that of the other MOS transistors are $W = 4 \mu\text{m}$. So n is equal to 2 in (3). The supply voltages are $V_{DD} = -V_{SS} = 1.5 \text{ V}$. The bias currents of OTA are $I_{B1} = I_{B2} = 80 \mu\text{A}$, and the bias currents of MO-CCCA are $I_A = I_{B3} = 10 \mu\text{A}$, the capacitances are $C_1 = 1 \text{ nF}$, $C_2 = 2 \text{ nF}$ (In the IC, the capacitor of $\sim\text{nF}$ is a little large, which can be fabricated by the combination of capacitance multipliers [31] and capacitors in parallel). The simulation on OTA with a bias current of $80 \mu\text{A}$ shows that G_m would be $111.7 \mu\text{S}$. Then, the natural frequency and quality factor can be calculated as $f_0 = 12.58 \text{ KHz}$ and $Q = 0.707$ according to (9). Figure 8 shows the simulated frequency responses of the proposed filter.

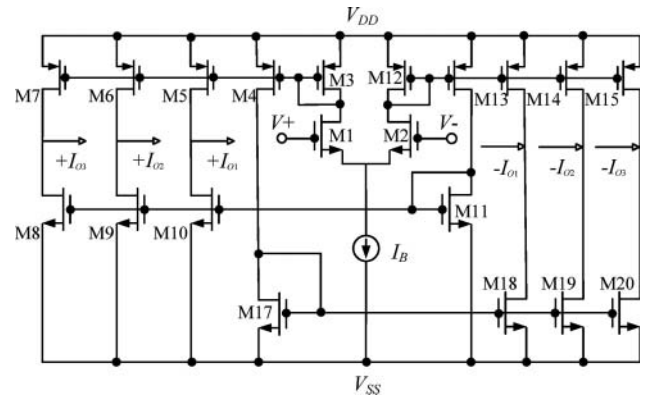


Figure 7: Realization circuit of OTA

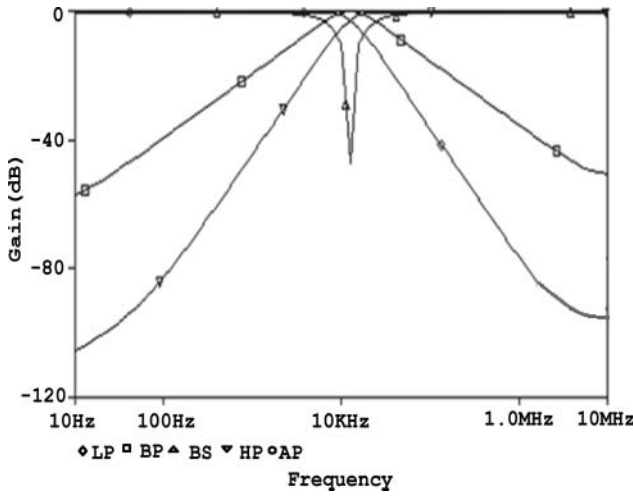


Figure 8: Frequency responses of the proposed filter

Figure 9 shows the simulated low-pass responses with f_0 ($f_0 = \omega_0/2\pi$)-tuning (i.e. $f_0 = 48.8$ KHz, 92.8 KHz, 125.8 KHz), while keeping $Q = 0.707$ invariant. In this case, the bias currents were $I_{B1} = I_{B2} = 10 \mu\text{A}$ ($G_m = 43.4 \mu\text{S}$), $40 \mu\text{A}$ ($G_m = 82.4 \mu\text{S}$) and $80 \mu\text{A}$ ($G_m = 111.7 \mu\text{S}$), $I_A = I_{B3} = 10 \mu\text{A}$, respectively, the capacitances are $C_1 = 0.1$ nF, $C_2 = 0.2$ nF.

Figure 10 shows the simulated band-pass responses with Q -tuning (i.e. $Q = 0.707, 1.0, 3.0$) keeping $f_0 = 125$ KHz. In this case, the capacitances are $C_1 = 0.1$ nF, $C_2 = 0.2$ nF, and the bias currents are $I_{B1} = I_{B2} = 80 \mu\text{A}$, $I_A = 10 \mu\text{A}$, and $I_{B3} = 10 \mu\text{A}, 7.07 \mu\text{A}, 2.36 \mu\text{A}$, respectively.

The analysis of the parasitic elements influence is validated with simulations by PSPICE. The simulations were done with variant I_{B1} and I_{B2} (e.g. $I_{B1} = I_{B2} = 50 \mu\text{A}, 80 \mu\text{A}$), while keeping $I_A = I_{B3}$, and $2C_1 = C_2 = 0.2$ nF. Simulations show that the transconductance of OTA with a bias current of $50 \mu\text{A}$ would be 91.08 and $111.75 \mu\text{S}$, with a bias current of $80 \mu\text{A}$, so the natural frequency f_0

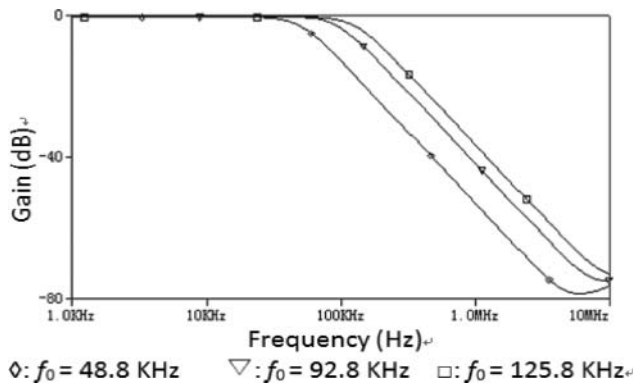


Figure 9: Simulated low-pass responses of the filter with f_0 -tuning

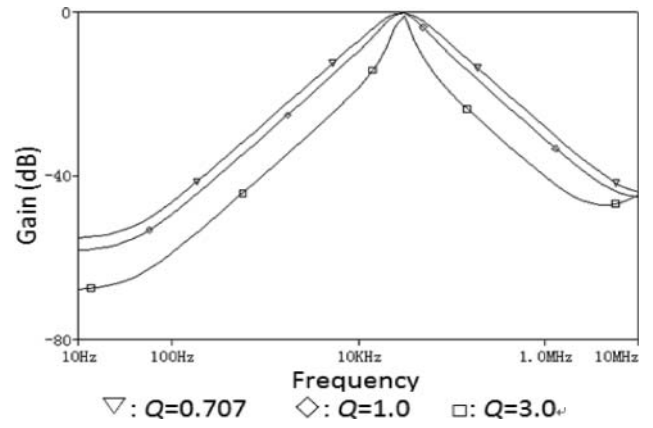


Figure 10: Simulated band-pass responses of the filter with Q -tuning

can be calculated as $f_0 = 102.561$ KHz, 125.826 KHz in the ideal condition, respectively. Figure 11 shows the simulated frequency response compared with the ideal results, Figure 11(a) shows the results with $I_{B1} = I_{B2} = 50 \mu\text{A}$, it can be seen that the simulated f_0 is turned to be 102.920 KHz, which is 359 Hz higher than the one in the

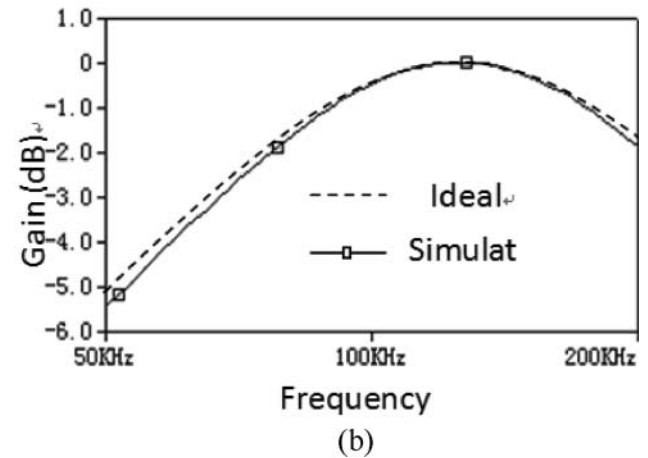
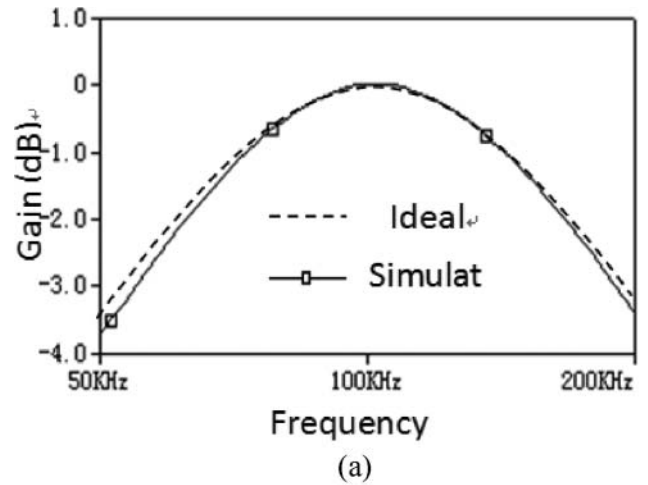


Figure 11: Simulated frequency response compared with the ideal results (a) $I_{B1} = I_{B2} = 10 \mu\text{A}$; (b) $I_{B1} = I_{B2} = 40 \mu\text{A}$

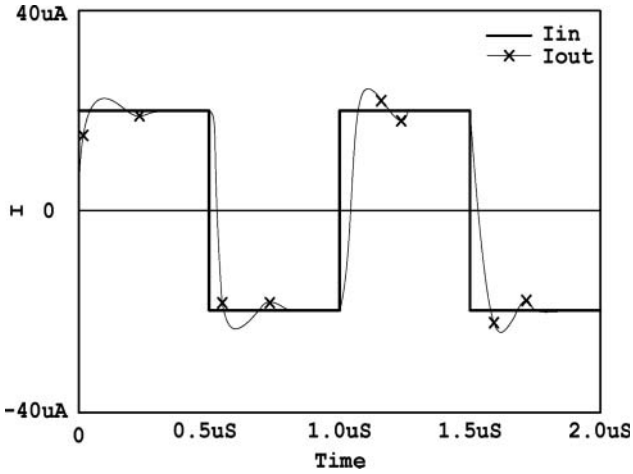


Figure 12: Square waveforms transient response of the proposed LP filter

ideal condition, in addition, Q is also higher than the ideal one. Figure 11(b) shows the frequency response with $I_{B1} = I_{B2} = 80 \mu\text{A}$, the simulated f_0 is 125.893 KHz, which is slightly higher than the one in the ideal condition, moreover, Q is also higher than the ideal one. Therefore, the analysis on the parasitic elements influence is verified.

The time-domain response of proposed low-pass filter is shown in Figure 12. The input I_{in} is square wave signal (with amplitude of $20 \mu\text{A}$, the frequency of 1 MHz). This result confirms that the switching delay time of the filter is approximately 1 ns.

To test the large signal behaviour of the presented filter, the circuit's total harmonic distortion (THD) analysis is made in Figure 13 (sinusoidal current at 1 MHz as input signal). According to Figure 13, the circuit's THD is less

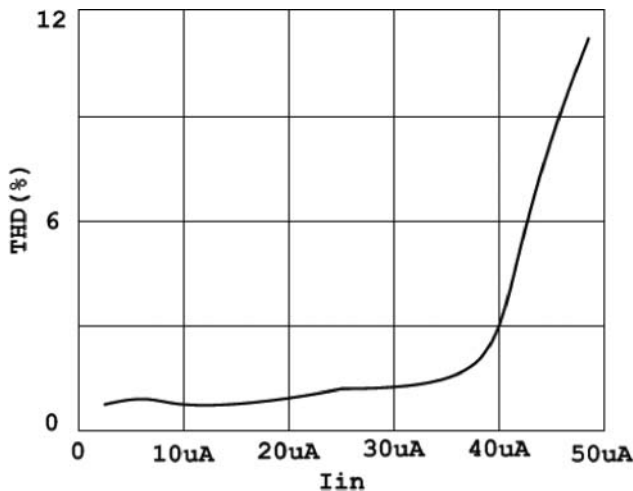


Figure 13: Total harmonic distortion of the filter

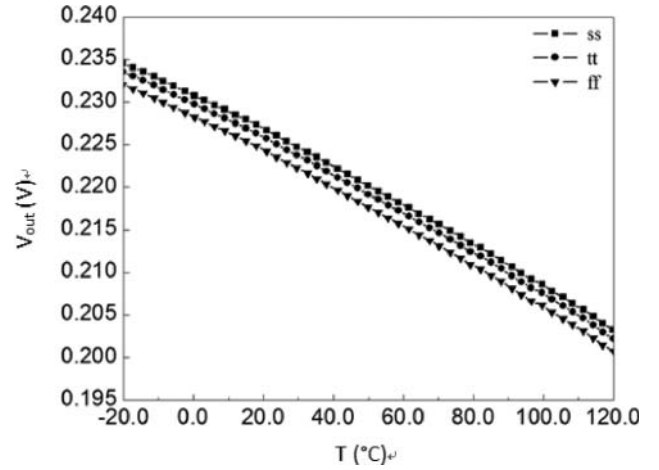


Figure 14: The change of V_{out} with different corners (ss, tt, and ff)

than 3% when current amplitude does not exceed $40 \mu\text{A}$. Considering the effect of process voltage temperature (PVT), we utilize the low-pass filter to simulate. Figure 14 shows the change of V_{out} (the voltage of port I_{o1}) which is produced with different corners (ss, tt, and ff). In Figure 14, the temperature is changed from -20 to $120 \text{ }^\circ\text{C}$, and the V_{out} is changed by 35 mV.

6. CONCLUSION

The paper presents a new OTA-C current-mode second-order filtering circuit with SIMO by introducing a MO-CCCA. The circuit has the following merits: (1) it has simple circuit structure which just contains three active components and two grounded capacitors; (2) it can simultaneously realize second-order low-pass, band-pass, high-pass, band-stop, and all-pass filters; (3) the natural frequency and the quality factor are independently tunable; (4) all-passive elements are all grounded, it is convenient to integrate; (5) it enjoys very low sensitivities.

Acknowledgment

Authors thank the anonymous reviewers for their contribution to the improvements of this paper.

DISCLOSURE STATEMENT

No potential conflict of interest was reported by the authors.

FUNDING

The authors would like to thank the National Natural Science Foundation of China [grant number 61571185]; Natural

Science Foundation of Hunan Province, China [grant number 2016JJ2030]; Open Fund Project of Key Laboratory in Hunan Universities, China [grant number 15K027].

REFERENCES

1. L. Sen, J. Jinguang, Z. Xifeng, and Z. Zeyu, "A novel current-mode versatile filter employing CCCDCC and MO-OTA," in *Proceedings of the IEEE 10th International Conference on ASIC*, Shenzhen, Oct. 2013, pp. 28–31.
2. C. C. Hsu and W. S. Feng, "Structural design of current-mode biquad filters," *Int. J. Electron.*, Vol. 88, no. 1, pp. 41–51, Jan. 2001.
3. B. Al-hashimi, "Current mode filter structure based on dual output transconductance amplifiers," *Electron. Lett.*, Vol. 32, no. 1, pp. 25–6, Jan. 1996.
4. M. T. Abuelma'atti and H. A. Alzahr, "Universal three input and one output current-mode filter without external passive elements," *Electron. Lett.*, Vol. 33, no. 4, pp. 281–3, Feb. 1997.
5. C. Chun-ming, "New multifunction OTA-C biquads," *IEEE Trans. Circuits Syst. II-Analog Digit. Signal Process.*, Vol. 46, no. 6, pp. 820–4, Jun. 1999.
6. S. Yichuang, "Design of current-mode multiple output OTA and capacitor filters," *Int. J. Electron.*, Vol. 1, no. 1, pp. 95–9, Jul. 1996.
7. C. Chun-ming and P. Shih-kuang, "Universal current-mode OTA-C biquad with the minimum components," *IEEE Trans. Circuits Syst. I-Fundam. Theor. Appl.*, Vol. 47, no. 8, pp. 1235–8, Aug. 2000.
8. S. Yichuang and J.K. Fidler, "Structure generation of current-mode two integrator loop dual output-OTA grounded capacitor filters," *IEEE Trans. Circuits Syst. II-Analog Digit. Signal Process.*, Vol. 43, no. 9, pp. 659–63, Sep. 1996.
9. T. Tsukutani, M. Higashimura, Y. Sumi, and Y. Fukui, "Electronically tunable current-mode biquad using OTAs and grounded capacitors," *IEICE Trans. Fundam. Electron. Commun. Comput. Sci.*, Vol. E84A, no. 10, pp. 2595–9, Oct. 2001.
10. Z. Xifeng, L. Shanahan, and W. Jiake, "An electronically tunable active-C current-mode universal filter employing CCCII and OTA," in *Proceedings of the IEEE 2011 Computer Science and Automation Engineering*, Vol. 4, Shanghai, Jun. 2011, pp. 647–51.
11. Q. Abdul Talat and A. Talat, "Current mode canonic OTA-C universal filter with single input and multiple outputs," in *Proceedings of the IEEE 2010 International Conference on Electronic Computer Technology*, Kuala Lumpur, May 2010, pp. 281–3.
12. S. Yasuaki, T. Takao, T. Hideki, and Y. Noboru, "Electrical tunable multiple-mode universal biquadratic circuits," in *Proceedings of the IEEE 2010 International Conference on Computer Applications and Industrial Electronics*, Kuala Lumpur, Dec. 2010, pp. 387–90.
13. K. V. Dattaguru, "TO-OTA based current-mode biquad filters," *Trans. Eng. Sci.*, Vol. 2, pp. 15–26, Aug. 2014.
14. T. Tsukutani, "Versatile current-mode biquad filter using multiple current output OTAs," *Int. J. Electron.*, Vol. 80, no. 4, pp. 533–41, Apr. 1996.
15. W. Jie and E. El-masry, "Universal voltage- and current-mode OTAs based biquads," *Int. J. Electron.*, Vol. 85, no. 5, pp. 553–60, Feb. 1998.
16. T. Tsukutani, Y. Sumi, M. Higashimura, and Y. Fukui, "Current-mode biquad using OTAs and CF," *Electron. Lett.*, Vol. 39, no. 3, pp. 262–3, Feb. 2003.
17. C.-M. Chang, B. Al-hashim, and J. N. Ross, "Unified active filter biquad structures," *IEE Proc.-Circuit Device Syst.*, Vol. 151, no. 4, pp. 273–7, Aug. 2004.
18. N. A. Shah and M. A. Malik, "High impedance voltage-mode and current-mode multifunction filters," *AEU-Int. J. Electron. Commun.*, Vol. 59, no. 4, pp. 262–6, Mar. 2005.
19. T. Tsukutani, Y. Sumi, and Y. Fukui, "Electronically tunable current-mode OTA-C biquad using two integrator loop structure," *Frequenz*, Vol. 60, no. 4, pp. 5356, Apr.–Mar. 2006.
20. T. Tsukutani, S. Edasaki, Y. Sumi, and Y. Fukui, "Current-mode Universal biquad filter using OTAs and DO-CCII," *Frequenz*, Vol. 60, no. 11–12, pp. 237–40, Nov.–Dec. 2006.
21. D. V. Kamat, P. V. Mohan, and K. G. Prabhu, "Novel first-order and second-order current-mode filters using multiple-output operational transconductance amplifiers," *Circuits Syst. Signal. Process.*, Vol. 29, no. 3, pp. 553–76, Jun. 2010.
22. W. Chunhua, X. Jing, A. U. Keskin, D. Sichun, and Z. Qiuqing, "A new current-mode current-controlled SIMO-type universal filter," *AEU-Int. J. Electron. Commun.*, Vol. 65, no. 3, pp. 231–4, Mar. 2011.
23. W. Chunhua, L. Haiguang, and Z. Yan, "A new current-mode current-controlled universal filter based on CCCII," *Circuits Syst. Signal. Process.*, Vol. 27, no. 5, pp. 673–682, Oct. 2008.
24. W. Chunhua, Z. Yan, Z. Qiuqing, and D. Sichun, "A new current-mode SIMO-type universal biquad employing multi-output current conveyors (MOCCIs)," *Radioengineering*, Vol. 18, no. 1, pp. 83–8, Apr. 2009.
25. W. Chunhua, Z. Lin, and L. Tao, "A new OTA-C current-mode biquad filter with single input and multiple

outputs,” *AEU-Int. J. Electron. Commun.*, Vol. 62, no. 3, pp. 232–4, Mar. 2008.

26. Y. Erkan, M. Bilgin, and C. Oguzhan, “Current-mode biquadratic filters using single CCII and minimum numbers of passive elements,” *Frequenz*, Vol. 58, no. 9–10, pp. 225–8, Sep.–Oct. 2004.
27. W. Chunhua, L. Haiguang, and Z. Yan, “Universal current-mode filter with multiple inputs and one output using MOCCII and MO-CCCA,” *AEU-Int. J. Electron. Commun.*, Vol. 63, no. 6, pp. 448–53, Nov. 2009.
28. B. Klaas and W. Hans, “A class of analog CMOS circuits based on the square-law characteristic of a CMOS,” *IEEE J. Solid-State Circuit.*, Vol. 22, no. 3, pp. 357–65, Jun. 1987.
29. B. Razavi, *Design of Analog CMOS Integrated Circuits*. New York: McGraw-Hill, 2001, pp. 28–46.
30. J. Ramirez-angulo, M. Robinson, and E. Sanchez-sinocio, “Current mode continuous time filters two design approaches,” *IEEE Trans. Circuits Syst. II-Analog Digit. Signal Process.*, Vol. 39, no. 6, pp. 337–41, Jun. 1992.
31. I. Padilla-Cantoya, “Capacitor multiplier with wide dynamic range and large multiplication factor for filter applications,” *IEEE Trans. Circuits Syst. II-Express Briefs*, Vol. 60, no. 3, pp. 152–6, Mar. 2013.

APPENDIX

The small-signal equivalent circuit of MO-CCCA input stage is shown in Figure 1(a), and it can be transformed to Figure 1(b), where $Z_1 = \frac{1}{g_{ds1} + sC_1'}$, $Z_2 = \frac{1}{g_{ds2} + sC_3'}$, $Z_3 = \frac{1}{sC_2'}$, then the following functions can be obtained:

$$i_{in} = g_{m1}v_{in} + i_1 + i_2 = g_{m1}i_1Z_1 + i_1 + i_2 \quad (A1)$$

$$v_{in} = i_2Z_3 - i_{in}'R_L \quad (A2)$$

$$i_2 = g_{m2}v_{in} + i_3 - i_{in}' \quad (A3)$$

$$i_3 = -i_{in}'R_L/Z_2 \quad (A4)$$

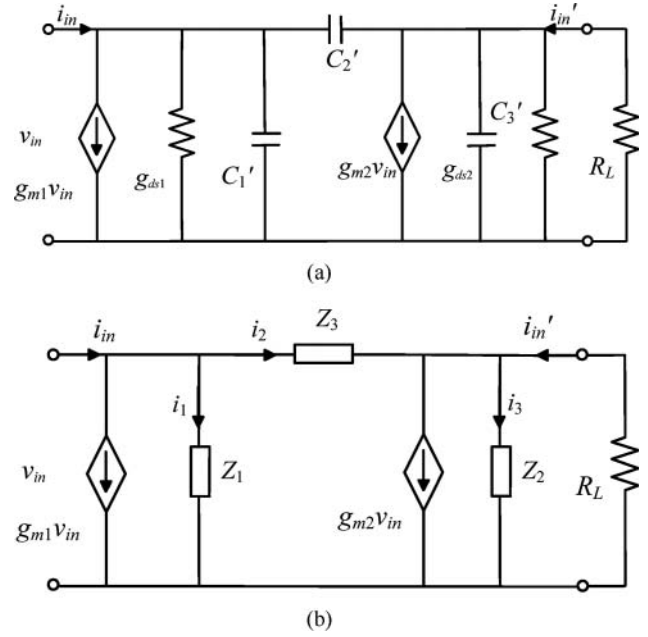


Figure A1: Small-signal equivalent circuit of MO-CCCA input stage

From the above equations, we can obtain

$$i_{in} = \frac{i_{in}' \left[(R_L + Z_2) \frac{Z_3}{Z_2} + R_L \right]}{Z_1(Z_3g_{m2} - 1)} (1 + Z_1g_{m1}) + \frac{i_{in}'}{Z_3} \left[\frac{(R_L + Z_2) \frac{Z_3}{Z_2} + R_L}{(Z_3g_{m2} - 1)} + R_L \right] \quad (A5)$$

For the sake of simple, R_L is assumed to be very small, so the current gain can be written as

$$\frac{i_{in}'}{i_{in}} = \frac{Z_1(Z_3g_{m2} - 1)}{Z_3(1 + Z_1g_{m1}) + Z_1} \quad (A6)$$

Replacing Z_1 , Z_2 , and Z_3 with their expressions, then

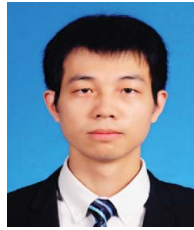
$$\frac{i_{in}'}{i_{in}} = \frac{g_{m2} - sC_2'}{s(C_1' + C_2') + g_{m1} + g_{ds1}} \quad (A7)$$

Authors



Yi Li was born in Taoyuan, China, in 1975. He is currently studying in Hunan University for the PhD degree. His research areas are focused on RF *circuits and analogue IC circuit design*.

E-mail: 466944824@qq.com



Baihui Zhu received the BS degree in 2014. He is currently studying in Hunan University for master degree. His research areas are mainly in analogue IC circuit and current-mode filter design.

E-mail: 506709196@qq.com



Chunhua Wang was born in Yongzhou, China, in 1963. He received the PhD degree from Beijing University of Technology, Beijing, China. He is currently a professor of Hunan University, Changsha, China. His research includes current-mode circuit design and RFIC design. He is the corresponding author.

E-mail: wch1227164@hnu.edu.cn



Zhenhua Hu was born in Chenzhou, China, in 1980. He is currently studying in Hunan University for the PhD degree. His research interests are mainly in wireless communication circuit, ultra-low power, and ultra-wideband RFIC design.

E-mail: huding86196125@163.com
